

Corrosion Resistance of the Ni-Mo Alloy Coatings Related to Coating's Electroplating Parameters

Pao-Chang Huang¹, Kung-Hsu Hou^{2,}, Gao-Liang Wang^{3,*}, Mao-Lin Chen⁴, Jee-Ray Wang⁴*

¹School of Defense Science, Chung Cheng Institute of Technology, National Defense University, Taoyuan, Taiwan

²Department of Power Vehicle and Systems Engineering, Chung Cheng Institute of Technology, National Defense University, Taoyuan, Taiwan

³ Department of Marketing Management, Takming University of Science and Technology, Taipei, Taiwan

⁴ Department of Automation Engineering & Institute of Mechatronoptic, Chienkuo Technology University, Changhua, Taiwan

*E-mail: khoucloud@gmail.com; khou@ndu.edu.tw; wanggl@takming.edu.tw

Received: 3 March 2015 / Accepted: 7 April 2015 / Published: 28 April 2015

The preparation of Ni-Mo alloy coating by pulse current technology was discussed in this study. We adjusted the bath composition in citric acid-ammonia solution, and changing different parameters such as duty cycle and pulse frequency to obtain different property of Ni-Mo coating. This study investigated the coatings properties that including element variations, corrosion resistance, mechanical properties, etc. all were related to deposited parameters. Scanning Electronic Microscopy (SEM) was used to observe the surface morphology and microstructure of the coatings. The compositions of the coatings were analyzed by EPMA. Linear polarization analysis coating polarization curve was used to recognize corrosion resistance. The experimental results showed that Ni-Mo alloys coatings by pulse current (PC) plating have better corrosion resistance than the direct current (DC) plating on the same current density. The optimal parameters are duty cycle 0.7 and frequency 1000 Hz. Ni-Mo composite coating with Mo content 30.2 wt% is obtained with the highest corrosion resistance.

Keywords: Electrodeposition, Ni–Mo alloy, Pulse current, Hardness, Corrosion resistance.

1. INTRODUCTION

Due to the increased demand for surface modification technology in recent years, a variety of functional coatings are widely used in various fields of electronics, automotive, aerospace, molding and chemicals industry. Because of hexavalent hard chromium plating with the high hardness, good

corrosion resistance, good gloss and low cost characteristics, so it is often applied on the relevant functional mechanical parts. However, Waste Electronics and Electrical Equipment Directive (WEEE Directive) and Restriction of Hazardous Substance Directive (RoHS Directive) have banned the use of toxic and carcinogenic hexavalent chromium plating. The development of one series alternative protective coatings are mainly nickel-based alloy coatings, such as Ni-Fe, Ni-Co, Ni-P, Ni-W, Ni-Mo alloys. Wherein the Ni-Mo alloy have excellent properties including high hardness and strength, suitable wear resistance, good corrosion resistance, and high thermal resistance[1]. If we can use its excellent performance to become functional protective coating, it has the opportunity to replace hexavalent chromium surface coating.

In literatures, co-deposition of nickel ion with molybdate ions is mostly used in citric acid - ammonia bath conditions and show the best complexing agent is sodium citrate together with ammonia[2,3]. The electrodeposited Ni-Mo alloy coatings have excellent mechanical properties making them exhibit potential as a replacement for hard chrome. In addition, they also have high electrochemical activity and lower costs, that makes the Ni-Mo alloys are gradually used in modern electrochemical industries[4-6]. Another potentially used feature is the Ni-Mo alloy with low hydrogen over potential so it is a suitable material for hydrogen production reaction[3, 7-10].

Many previous studies have investigated the corrosion properties of DC plating Ni-Mo alloy. Lima-Neto et al. [11] reported on the effect of heat treatment on the structure and corrosion characteristics of electrodeposited Cr and Ni-Mo coatings. As the annealing temperature rises, Ni-13 wt.% Mo plating layer has good corrosion resistance due to reinforcement of coating mechanical property by the precipitation of Ni₄Mo and NiMo phases. Halim et al. [12] explored the corrosion resistance of DC plating Ni-Mo coating with different Mo content (11 wt.%~31wt.%) in 0.5M NaOH aqueous solution. The results show the Ni-Mo coatings at Mo content 15.1wt.% with electrochemical corrosion current (I_{corr}) $4.06\mu A/cm^2$ showing the best corrosion resistance in their study. The high Mo content (31wt.%) coating with low corrosion resistance that was because of the coating cracks introduced by high internal stresses. Niedbala [13] compared the corrosion resistance of Ni-10wt.% Mo alloy, Ni-10wt.% Mo-P alloys and Ni+10% Mo composite coating, it shows the Ni-10wt.% Mo alloy have good corrosion resistance(I_{corr} : $0.35\mu A / cm^2$) than Ni-10wt.% Mo-P alloy (I_{corr} : $0.92\mu A / cm^2$) and Ni + 10% Mo composite coatings (I_{corr} : $0.18mA / cm^2$).

In order for the Ni-Mo alloy coating to have better corrosion resistance, this study imported pulse current (PC) plating. PC plating is unlike direct current (DC) plating, that is attributed to the pulse current parameters changes the diffusion layer and the transfer structure [14, 15]. In general, it can modify the coating surface morphology and structure by controlling the PC plating parameters, and enhance the coating properties [16, 17]. As a result, the effects of PC electrodeposition parameters on the microstructure and properties of metals and alloys have been reported in many literatures. But for the PC plating nickel-molybdenum alloy coatings related research is still limited.

Cherkaoui et al.[18], obtained a compact and crack-free Ni-Mo coating layer from electrodeposition of pulse current. Their study shows that the Mo content in the coating mainly depends on the pulse current density as at high duty cycles condition. At low duty cycles condition, both the deposit composition and morphology are influenced by the pulse relaxation durations. Marlot et al. [9] illustrated that the Ni-Mo coatings composition and the current efficiency were measured as a

function of pulse current parameters (pulse period, duty cycle) and mass transport parameters (electrode rotation speed, molybdate concentration). At sufficiently short pulse periods (less than 10s), the Mo content of the PC plated alloys was higher than in DC plating. Allahyazadeha et al.[19] research shows that the Ni–Mo alloy has been electrodeposited on mild steel in the presence of ionic liquid additive 1-ethyl-3-methyl-imidazolium chloride and in ammonia citrate solution using PC plating technique. And the Ni–Mo films containing more than 49 wt.% Mo in the presence of ionic liquid at pH of 8.5. Han et al.[20] report that the optimum electrodeposition conditions by PC plating with respect to Hydrogen evolution reaction (HER) over potential were determined. The amorphous Ni-Mo coating was obtained when the molybdenum content was 30 wt.%, which shows high HER activity and excellent corrosion resistance.

From the literatures, they show that the Ni-Mo coating produced by PC plating has good coatings properties, and may be with the potential to replace hexavalent chromium plating in industrial applications. However, the corrosion resistance and coatings properties related to the pulse current plating parameters for Ni-Mo coatings were seldom discussed. Therefore, this study was to investigate the co-deposition of mechanical properties and corrosion resistance of Ni-Mo alloy coating by changing the pulse plating parameters.

2. EXPERIMENTAL DETAILS

The Ni-Mo alloy were deposited in the solution which composition contains: nickel sulfate ($\text{NiSO}_4 \cdot 6\text{H}_2\text{O}$) 0.2 M, Sodium molybdate ($\text{Na}_2\text{MoO}_4 \cdot 2\text{H}_2\text{O}$) 0~0.04M, and Sodium citrate ($\text{Na}_3\text{C}_6\text{H}_5\text{O}_7$) 0.2M. The compositions and the range of experimental operating conditions are shown in Table 1.

Table 1. Composition of the electrolytic bath and operating conditions or Ni-Mo coatings.

Component	Concentration (mol/dm ³)
$\text{NiSO}_4 \cdot 6\text{H}_2\text{O}$	0.2
$\text{Na}_2\text{MoO}_4 \cdot 2\text{H}_2\text{O}$	0.04
$\text{Na}_3\text{C}_6\text{H}_5\text{O}_7$	0.2
Operating conditions	
pH	9.5
Temperature	30 °C
Current density	10 A/dm ²
Duty cycle	0.2~0.9
Frequency	10, 100, and 1000 Hz
Total charge deposition	5850 C

The pH value of the baths was adjusted to 9.5 using an ammonia solution. In the electroplating process, the temperature of plating bath was controlled at Celsius degree 30 °C and the magnetic stirrer

circulated at a speed of 250 rpm. Total fixed quantity of electricity is 5850 coulomb by DC/PC power supply (Model: MOTECH6000). Plating time ranges from 1 to 5 hours which is adjusted according to current density. The current regulates the on-off period, to yield symmetrical or asymmetrical electric cycle waves during the deposition. The pulse current parameters include the peak current density i_p , the charging time (T_{on}), the rest time (T_{off}), the duty cycle ($T_{on}/(T_{on} + T_{off})$) and the pulse frequency ($1/(T_{on} + T_{off})$).

The Ni-Mo coatings were plated on steel substrate (size of 33mm x 50mm), which was prepared by degreasing in alkaline soak solution (NaOH 1M, 60 °C), pickled in hydrochloric acid (HCl 30%) and finally cleaned with deionized water, and thus completed the plating specimen preparation. After plating, the samples were cut into small area of 1 cm² using the abrasive cutting machine (TNC-50B, Neyagawa) for the purpose of morphology, microstructure, and composition analysis. The surface microstructure as well as cross sections of the coatings was observed by scanning electron microscopy (SEM, Jeol model JSM-6500). Measurement of surface roughness is by roughness detector (Japan SURFCORDER SE1700), and the mean value for the roughness (Ra) is calculated with 3 tests. The microstructure of the Ni-Mo deposit was also studied using a transmission electron microscope (TEM, JEOL-JEM2000FXII) operated at 100 kV. A thin sample for TEM observation was mechanically grounded with sandpaper and thinned by chemically polishing in sulfuric acid solution. The composition of sulfuric acid solution is 33% sulphuric acid and 67% water, then controlling the temperature at -20 °C in the process of chemical polishing. Micro structure of the Ni–Mo coatings was investigated using a X-ray diffractometer (XRD, Bruker D2 PHASER). Compositional analysis of Mo content in the coatings and line scan analysis were realized by applying Electron Probe X-ray Microanalyzer (EPMA, JXA-8200). Vickers micro-hardness tester (HVS-1000) was used to measure the hardness and the mean value for the hardness is calculated with 5 tests, loading with 50 g for 10 seconds.

Linear polarization testing was performed using a three-pole system (counter electrode, reference electrode and the working electrode) to assess the corrosion resistance of the coating. With 3.5% NaCl solution electrolyte and detection area of 1 cm², corrosion impedance tester (Potentiostat / Galvanostat Model 263A) was used to analyze the corrosion resistance of the coating—with scanning speed of 1 mV/s and polarization curves were used to analyze the corrosion voltage and corrosion current by the tafel slope.

3. RESULTS AND DISCUSSION

Fig. 1 shows the SEM images of two Ni-Mo deposits prepared by DC plating (a) and PC plating (b), respectively. The Ni-Mo coatings in this investigation demonstrated a nodular structure. When the coating was prepared by DC plating with current density 10ASD, the surface has a more severe nodular structure with the average surface roughness Ra, 2.26μm. However, when the coatings by PC plating with current density 10 ASD, duty cycle 0.7, frequency 100 Hz, the nodule size was diminished and the average surface roughness is Ra 1.23 μm. In DC plating, metal ions approaching the cathode are deposited continue constantly resulting in the hydrogen evolution and concentration

polarization were increased. As for PC plating process, metal ions approaching the cathode were fully deposited in the T_{on} while backing to the initial concentration in the T_{off} . Unlike DC plating, small grains and low porosity can be achieved with metal ions deposited under high over-potential [20, 21]. Therefore, pulse current plating will significantly affect the surface morphology smooth of Ni-Mo alloy coating.

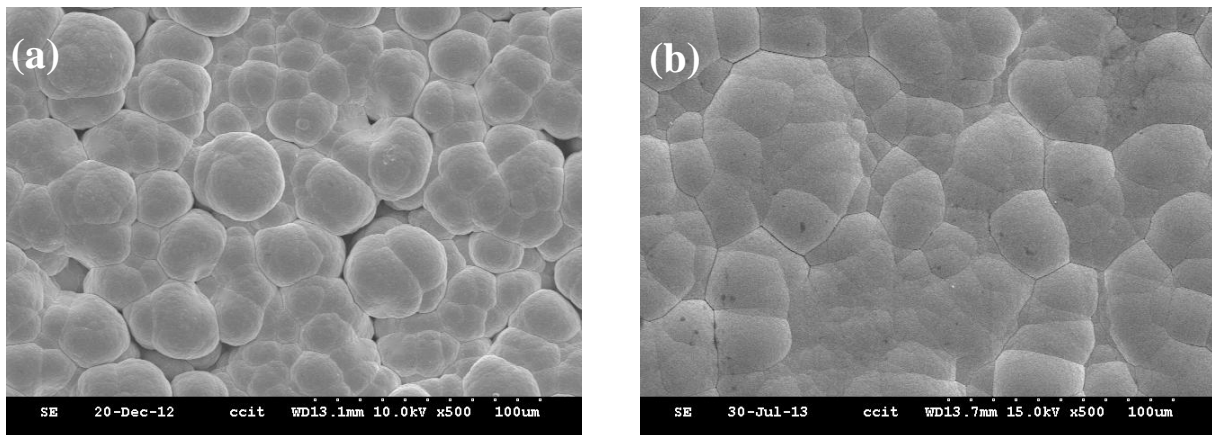


Figure 1. SEM images of the surface morphology: (a) DC 10 ASD, (b) PC 10 ASD, Duty cycle 0.7, Frequency 100 Hz.

3.1. Influence of duty cycle

Fig. 2 shows the SEM images of Ni-Mo deposits to render the effect of duty cycle variation.

The surface is undulating when the duty cycle is 0.9 (Fig. 2a). The surface morphology is indifferent with DC plating. With duty cycle 0.7(Fig. 2b), the surface relief has a gentle trend; with duty cycle 0.5(Fig. 2c), the surface morphology to change into a fine nodular, but the surface begins to crack. This is due to the high Mo content that leads to excessive internal stress. When reducing the duty cycle to 0.2(Fig. 2d), the surface of Ni-Mo coating is flat but with more obvious cracks. With fixed peak current density and frequency, reducing duty cycle will make the average current density decreased which induces the deposition rate to slow down. The reducing growth rate of the metal leads to smooth surface. However, the coating cracks due to the high internal stress.

Fig. 3 shows the effect of the duty cycle on the current efficiency for the electroplated Ni-Mo alloys with a fixed current density of 10ASD and a pulse frequency of 10 Hz. It shows as duty cycle decreases from 1 to 0.7, the current efficiency decreased from 62.68% to 54.83%. When the duty cycle is reduced to 0.5, the current efficiency quickly reduced to 28.49%. The SEM image of surface morphology (Fig.2c) indicates that the nodular surface is not obvious due to the low current efficiency and the reduction rate of the metal ions is slowing. When the duty cycle is as low as 0.2, the current efficiency is close to 0. A similar result was reported by Marlot et al. in their study of pulse plating of Ni-Mo alloys from nickel-rich electrolytes[9]. Their result indicated that a thin and non-compact Ni-Mo coating with a relatively high Mo content was obtained when the plating was formed with a duty cycle of 0.2, and the current efficiency under the duty cycle of 0.2 was very low (less than 5%). This

finding might be ascribed to the fact that the lower duty cycle results in a longer T_{off} and more Mo ions supplied on the cathode surface. Higher concentrations of Mo ions result in a reduced current efficiency [21-24].

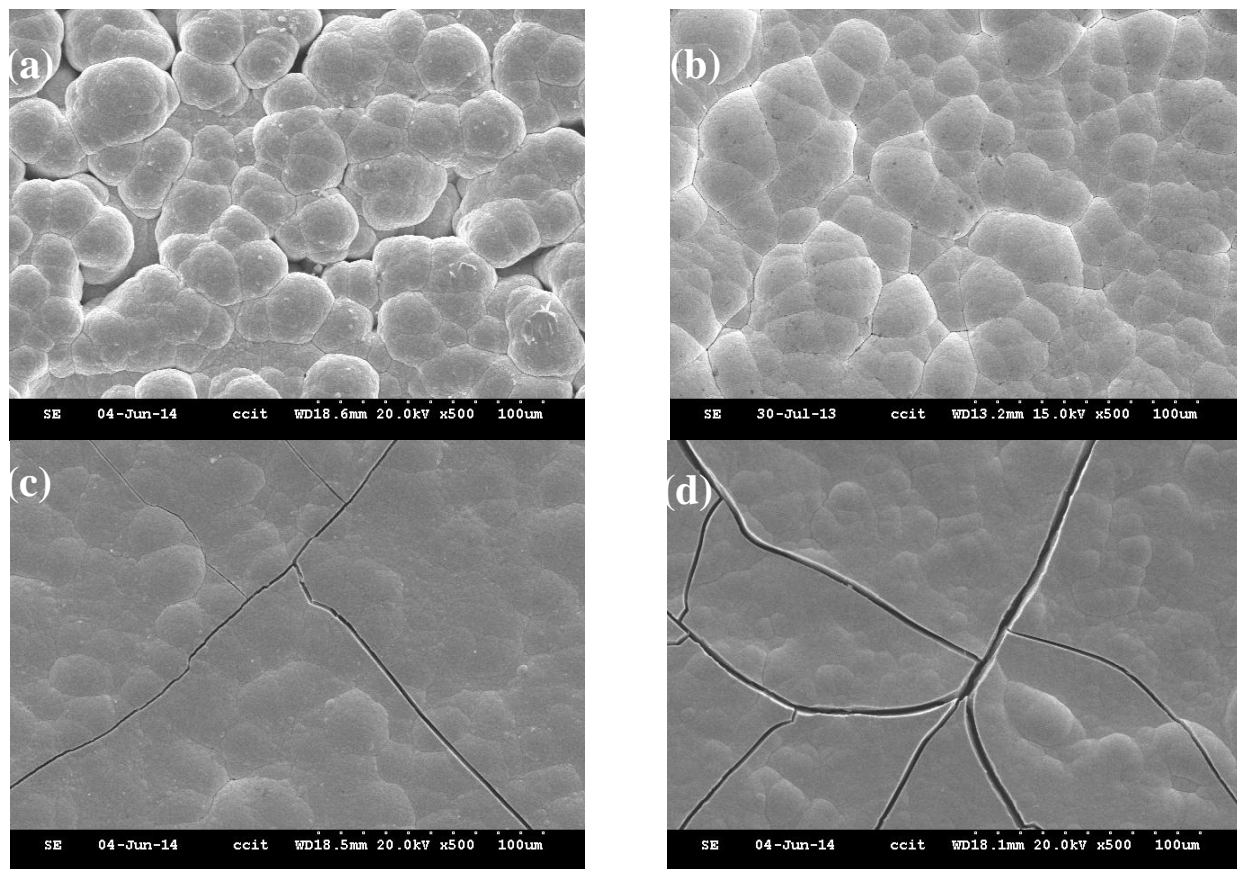


Figure 2. SEM images of the surface morphology: pulse plating current density 10 ASD, frequency 10 Hz, Duty cycle (a) 0.9 (b) 0.7 (c) 0.5 (d) 0.3

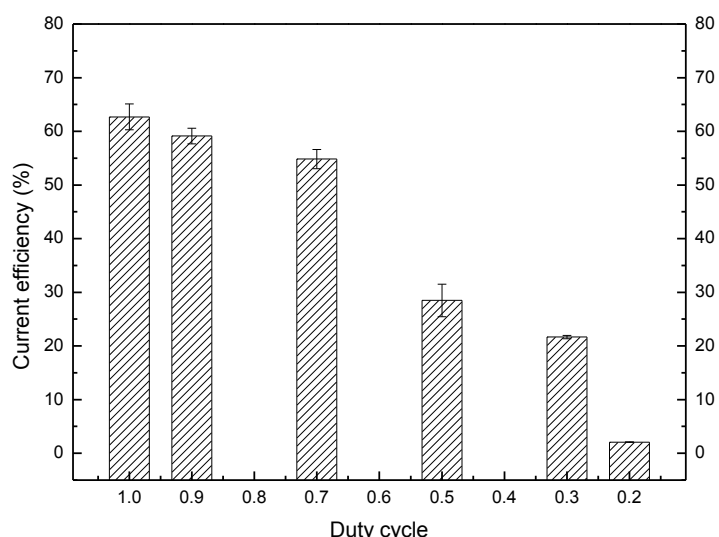


Figure 3. Effect of the duty cycle on the current efficiency (The concentration of molybdate = 0.04 M, current density = 10 ASD and frequency = 10 Hz).

3.2. Influence of Frequency

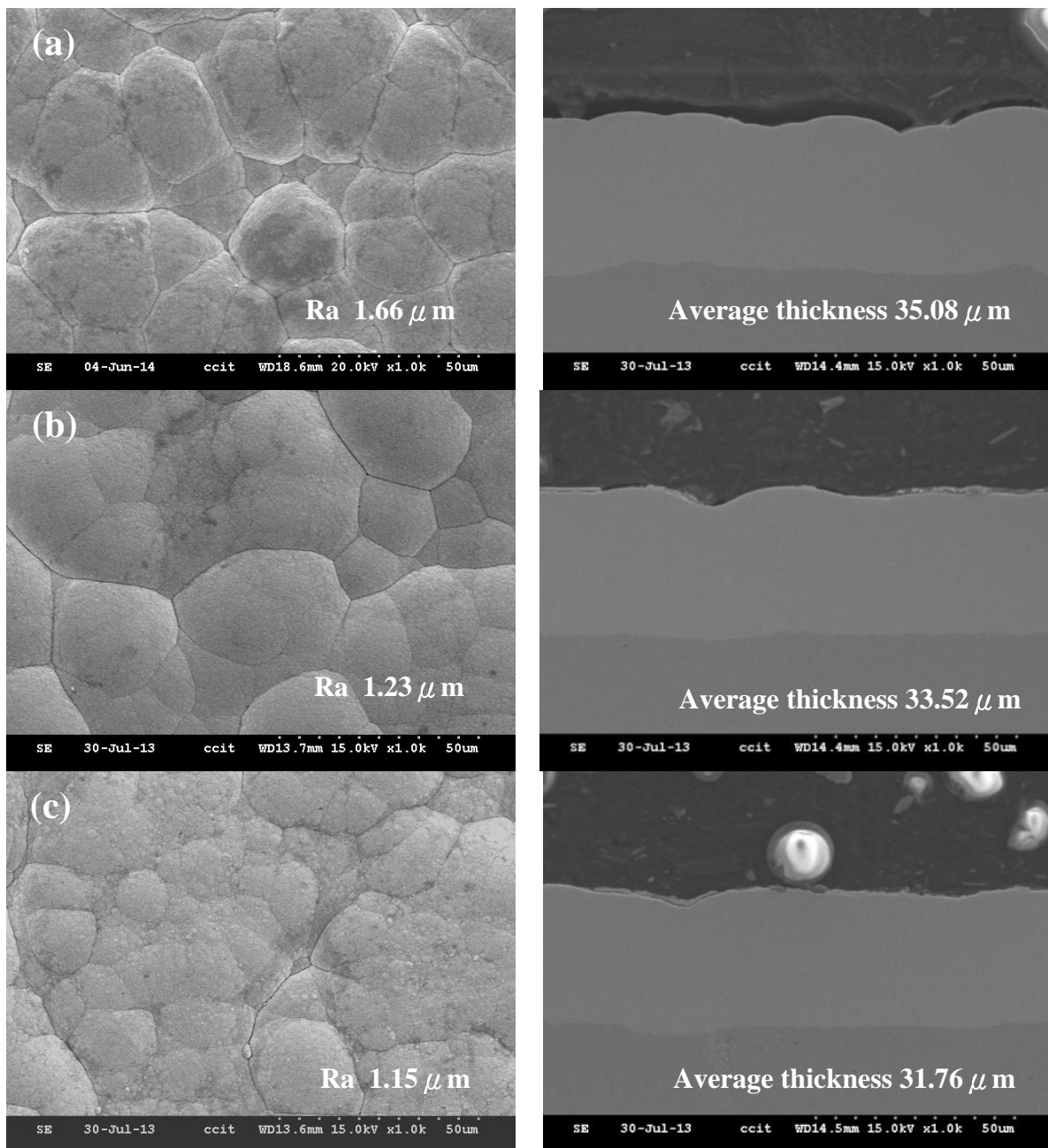


Figure 4. SEM images of the surface morphology and cross-section: pulse plating current density 10 ASD, duty cycle 0.7, and frequency (a) 10 Hz (b) 100Hz (c)1000Hz

Low duty cycle can easily lead to brittle of the coating, thus varying the pulse frequency and observe the microstructure by fixing the current density at 10 ASD and duty cycle at 0.7. Fig. 4 displaying the surface morphology and cross-sectional SEM images of the coatings which were produced by different pulse frequency. There are no cracks in this plating conditions and connected well to the substrate, therefore has a good protective properties. Fig. 4a is the surface morphology and cross-section of the coating at frequency 10 Hz. The surface relief is obvious compared to frequency at 100 Hz and 1000 Hz. When the frequency is increased to 100Hz, undulating is improved (Fig. 4b). At

pulse frequency 1000Hz, the coating surface is more smoothness (Fig. 4c). When the pulse frequency is increased from 10 Hz to 1000 Hz, the surface roughness of the coating was reduced from $1.66\mu\text{m}$ to $1.15\mu\text{m}$. Therefore, the surface morphology of the PC plating Ni-Mo coatings is significantly controlled by adjusting pulse frequency appropriately. As a result, the surface accuracy can be improved. From the cross-section of the coating, it is found that as pulse frequency increases from 10 Hz to 1000 Hz, coating average thickness reduces from $35.08\mu\text{m}$ to $31.76\mu\text{m}$.

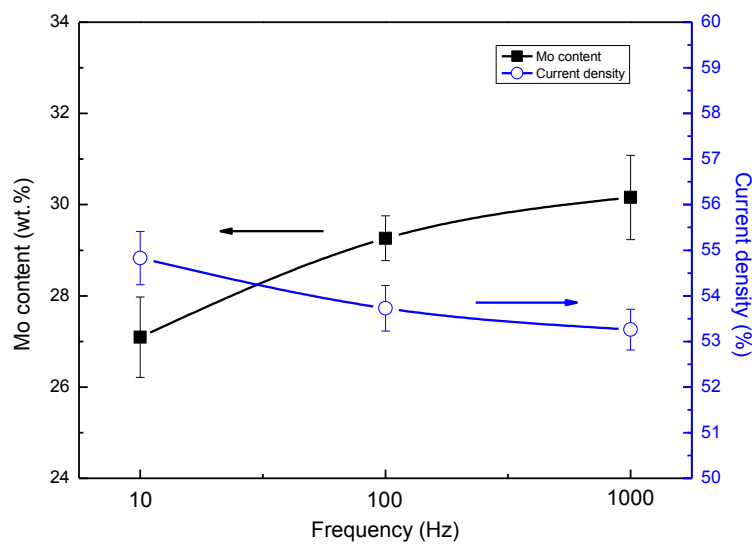


Figure 5. Effect of the frequency on the Mo content and current efficiency of the coating.

Fig. 5 shows the effects of frequency related to on the Mo content and current efficiency of the PC plating Ni-Mo coatings. It shows that as pulse frequency increases would result in current efficiency decreased, and the Mo content increased was caused by rise the frequency. This is due to the higher current efficiency at low frequency condition would be result in the nickel ions reduced rapidly than the molybdate ions, and leading to a relatively low Mo content exist in the coating.

3.3. Microstructure and Hardness of the coatings

To explore the effect of Mo content on the structure of pulse plating coating, a structural analysis of the deposits was performed using XRD. Fig. 6 shows the XRD pattern of the PC plating Ni-Mo coatings in this study. As the pulse frequency increase from 10 Hz to 1000Hz, Mo content of the coating increased from 27.09 wt.% to 30.16 wt.%, and the XRD diffraction peaks ($2\theta=44^\circ$) become increasingly broadened, and their intensities decrease. Numerous studies have emphasized that an increase of the Mo content in the coatings would result in the Ni-Mo coatings microstructure were gradually transform from a micro crystalline structure to a nanocrystalline/amorphous phase[21, 25-28]. In the same current density and duty cycle, the effect of the pulse frequency on Mo content is less, but it still follows such a trend same as above description. Fig. 7 is a TEM bright field image and electron diffraction pattern of Ni-30.16 wt.% Mo alloy coating. It can be observed that the grain size is less than 5 nm. The Selected Area Diffraction Pattern (SADP) presents the clear diffractive rings and

obvious diffractive points, so the nano crystal structure is confirmed. The grain size was calculated using Scherrer equation formula.

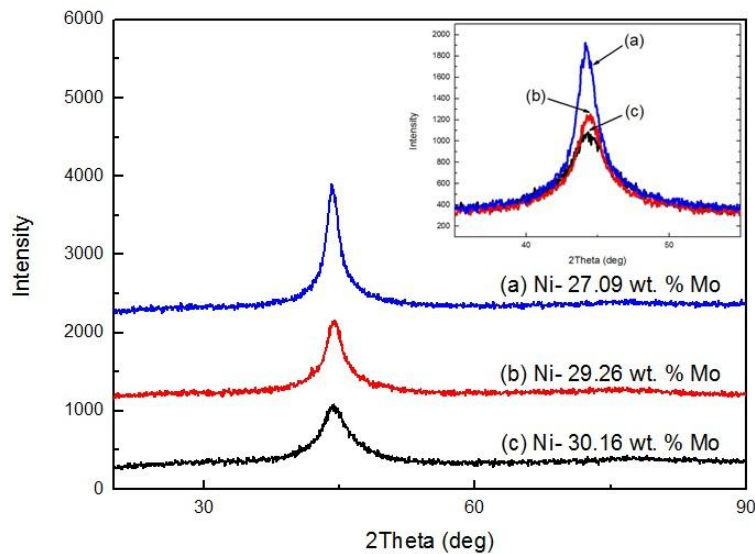


Figure 6. X-ray diffractograms for the as-electrodeposited Ni-Mo coatings. Plating conditions: current density = 10 ASD, duty cycle = 0.7 and frequency of (a) 10 Hz, (b) 100 Hz, and (c) 1000 Hz.

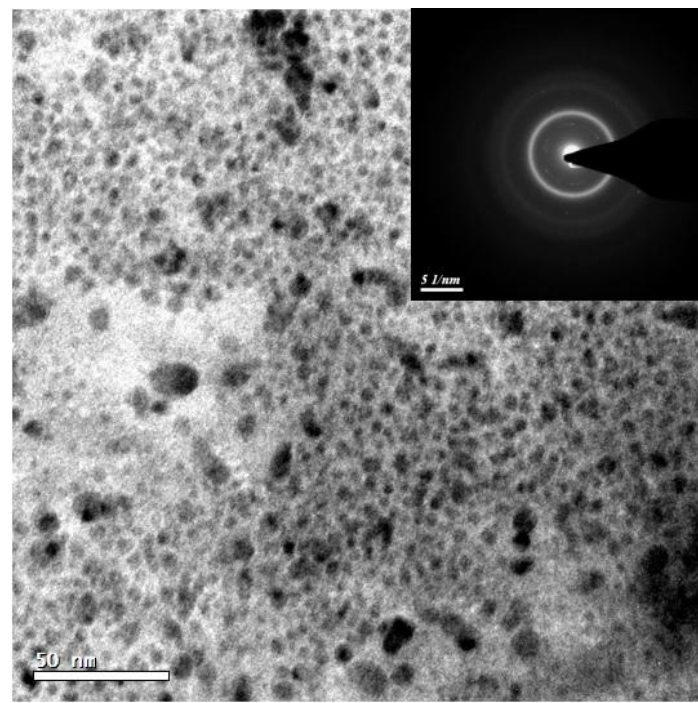


Figure 7. Bright-field TEM image and selected area electron diffraction of the Ni-Mo coating electroplated at 10 ASD, duty cycle = 0.7 and frequency = 1000 Hz.

As observed in Fig. 8, the grain size decreased (6.2 ~3.3 nm) was accompany with increasing the pulse frequency (10 Hz ~ 1000 Hz) that under the same condition at current density 10 ASD and duty cycle 0.7. And the enhancement of relative hardness of the coatings shows the presence of grain

refining strengthening. However, the grain size determined from TEM observations was slightly greater than that obtained from the XRD calculations based on Scherrer's equation. This result is consistent with literature reports[10, 26].

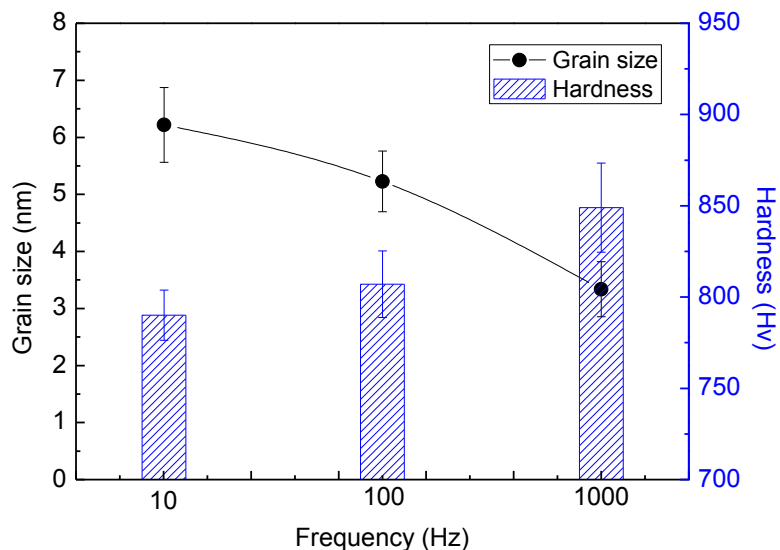


Figure 8. Effects of the frequency related to both of the grain size and hardness of the PC plating Ni-Mo coating.

In this study, the hardness of Ni-Mo alloy coating increased as the grain size decreases. Therefore the Ni-Mo alloy coating that produced by pulse plating still follow the Hall-Petch mechanism [29, 30], with maximum hardness up to 849 HV.

3.4. Corrosion Resistance with the polarization curves analysis

From the SEM surface morphology related to the duty cycle analysis. We are found that when the pulse duty cycle becomes as low as to 0.5, the coating surface will brittle and would be affect the corrosion resistance reduced. This is due to large internal stress caused by too high Mo content. Therefore, this section explores the corrosion resistance of the PC Ni-Mo coatings that are produced by current density 10 ASD, duty cycle 0.7, frequency 10~1000 Hz, and compared with the same current density DC Ni-Mo alloy plating and electroplating pure Ni plating. Fig. 9 presents the dynamic polarization curves of the coatings in 3.5%NaCl solution. The results show the PC 1000 Hz coating has the best corrosion resistance ($I_{corr}: 0.47\mu\text{A}/\text{cm}^2$), that is better than PC 100 Hz coating ($I_{corr}: 1.11\mu\text{A}/\text{cm}^2$) and PC 10Hz coating ($I_{corr}: 1.72\mu\text{A}/\text{cm}^2$). The corrosion resistance of high frequency coating (1000Hz) is 3.6 times for low frequency coating (10Hz). Moreover, compared to DC coating that produced by the same current density of 10 ASD ($I_{corr}: 3.31\mu\text{A}/\text{cm}^2$), the corrosion resistance of the PC 1000 Hz coating is 6.9 times for the DC coating, and 9.6 times for pure Ni plating. When the pulse plating Mo content is between 27.09 ~ 30.16 wt.%, Mo content of the coating has limited impact on

corrosion resistance (Table 2). This is discussed in the previous section that the pulse plating has a smooth modification effect on the coating surface morphology. So, the surface corrosion resistance has significantly improved as the deposition technique using the PC plating.

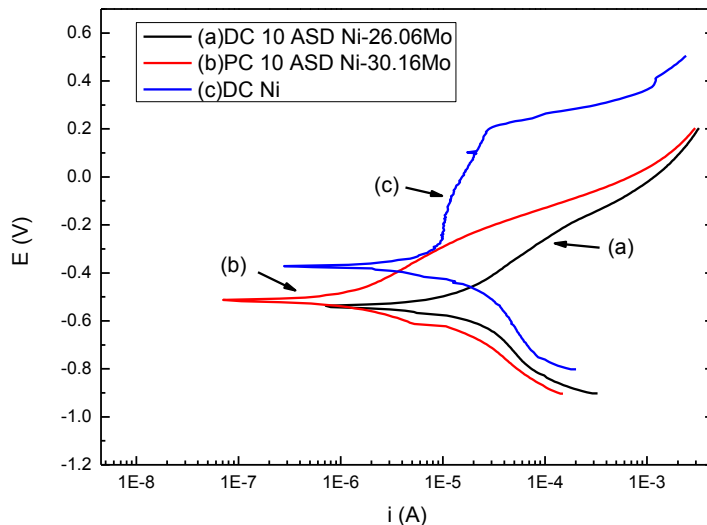


Figure 9. Polarization curves of the Ni-Mo and Ni coatings produced by DC and PC plating.

Previous research indicates that the corrosion behavior of the nano-crystals Ni-Mo alloy coating depends on two factors, the Mo content and grain size coating[12]. In this study, the corrosion behavior of PC plating Ni-Mo alloy is consistent with this argument.

Table 2. Experimental data of corrosion resistance of the Ni-Mo coatings.

Condition	Operating parameters			Mo content (wt.%)	Grain size (nm)	I_{corr} (A)	E_{corr} (V)
	Current density	Duty cycle	Frequency				
DC Ni-Mo	10	-	-	26.05	10.9	3.31×10^{-6}	-0.53
PC Ni-Mo	10	0.7	10	27.09	6.22	1.72×10^{-6}	-0.53
PC Ni-Mo	10	0.7	100	29.26	5.23	1.11×10^{-6}	-0.50
PC Ni-Mo	10	0.7	1000	30.16	3.34	4.77×10^{-7}	-0.51
DC Ni	10	-	-	-	25.27	4.57×10^{-6}	-0.37

Another, our study displaying the PC plating Ni-Mo coatings can provide a widely choice for more variation deposition conditions. As shown in Table 2, there is a tendency to enhance the corrosion resistance of the coating with the Mo content increases and the grain size reduces. Furthermore, in this research the PC plating technique provide an optimal operating condition choice related to the Ni-Mo coatings properties the including the surface morphology, microstructure, mechanical strength and the corrosion resistance.

4. CONCLUSIONS

In order to prepare a good corrosion resistance of pulse current (PC) deposited Ni-Mo alloy coating by using different PC plating parameters in this study. The relevant conclusions are as follows:

(1) The plating parameters of the coating influence the accuracy and smoothness of the coatings surfaces. This is one of the important indicators in components and precision machining processes. The study found that the surface morphology of Ni-Mo alloy coating can be improved by controlling pulse frequency and duty cycle.

(2) With lower duty cycle, the current efficiency decreases which is due to reduction in reaction inhibited by molybdate in cathode interface. Increasing the frequency in the range from 10-1000 Hz leads to increase in the Mo content in PC-plated coatings. The maximum Mo content (30.2 wt.%) in the coating occurred at a current density of 10 A/dm², a duty cycle of 0.7, and a frequency of 1000 Hz; this coating contained a microstructure that mixed with nanocrystalline and amorphous phase, which was according to the X-ray diffraction results and TEM analysis.

(3) The PC plating Ni-Mo coatings have grain size refined and with more smooth surface morphology, thereby improving corrosion resistance that was compared with the DC plating Ni-Mo coating. As the pulse frequency is increased, it can reduce the surface roughness and enhance the Mo content of the coating which further improves corrosion resistance. At current density 10ASD, duty cycle 0.7, frequency 1000Hz, $I_{corr} 4.77 * 10^{-7}$ (A / cm²), the best corrosion resistance is shown.

ACKNOWLEDGEMENT

The authors would like to thanks the financially supporting this research that come from the Ministry of Science and Technology of Taiwan under the following programs of No. NSC100-2221-E-606-007 and No. NSC 101-2221-E-606-006.

References

1. P. Prioteasa, L. Anicai, and T. Visan, *UPB Sci. Bull. Ser B*, 72 (2010) 11-24.
2. E. Chassaing, M. P. Roumegas, and M. F. Trichet, *J. Appl. Electrochem.*, 25(1995) 667-670.
3. L. S. Sanches, S. H. Domingues, A. Carubelli, and L. H. Mascaro, *J. Braz. Chem. Soc.*, 14 (2003) 556-563.
4. C. C. Hu and C. Y. Weng, *J. Appl. Electrochem.*, 30 (2000) 499-506.
5. W. Hu, X. Cao, F. Wang, and Y. Zhang, *Int. J. Hydrogen Energy*, 22 (1997) 621-623.
6. J. F. Kriz, H. Shimada, Y. Yoshimura, N. Matsubayashi, and A. Nishijima, *Fuel*, 74 (1995) 1852-1857.
7. Y. Zeng, Z. Li, M. Ma, and S. Zhou, *Electrochem. Commun.*, 2 (2000) 36-38.
8. F. A. Marinho, F. S. M. Santana, A. L. S. Vasconcelos, R. A. C. Santana, and S. Prasad, *J. Braz. Chem. Soc.*, 13 (2002) 522-528.
9. A. Marlot, P. Kern, and D. Landolt, *Electrochim. Acta*, 48 (2002) 29-36.
10. E. Chassaing, N. Portail, A.-f. Levy, and G. Wang, *J. Appl. Electrochem.*, 34 (2004) 1085-1091.
11. P. d. Lima-Neto, A. N. Correia, G. L. Vaz, and P. N. S. Casciano, *J. Braz. Chem. Soc.*, 21 (2010) 1968-1976.
12. J. Halim, R. Abdel-Karim, S. El-Raghy, M. Nabil, and A. Waheed, *J. Nanomaterials*, 2012 (2012) 18.

13. J. Niedbała, *Mater. Sci. Forum*, 514-516 (2006) 465-469.
14. D.-T. Chin, *J. Electrochem. Soc.*, 130 (1983) 1657-1667.
15. O. Chene and D. Landolt, *J. Appl. Electrochem.*, 19 (1989) 188-194.
16. J. C. Puippe and N. Ibl, *J. Appl. Electrochem.*, 10 (1980) 775-784.
17. L. G. Holmbom, *Plat. Surf. Finish.*, 74 (1987) 74-79.
18. M. Cherkaoui, E. Chassaing, and K. V. Quang, *Adv. Mater. Manuf. Processes*, 3 (1988) 407-418.
19. M. H. Allahyazadeh, B. Roodbehani, and A. Ashrafi, *Electrochim. Acta*, 56 (2011) 10210-10216.
20. Q. Han, S. Cui, N. Pu, J. Chen, K. Liu, and X. Wei, *Int. J. Hydrogen Energy*, 35 (2010) 5194-5201.
21. W. Coburn and W. Williams, *IEEE Trans. Magn.*, 31 (1995) 692-697.
22. E. Beltowska-Lehman and P. Indyka, *Thin Solid Films*, 520 (2012) 2046-2051.
23. U. S. Mohanty, B. C. Tripathy, P. Singh, S. C. Das, and V. N. Misra, *J. Appl. Electrochem.*, 38 (2008) 239-244.
24. E. Beltowska-Lehman, *Phys. Stat. Sol.*, 5 (2008) 3514-3517.
25. N. Li, W. Chen, B. Jing, and H. Xu, *Adv. Mat. Res.*, 148-149 (2011) 674-678.
26. E. Beltowska-Lehman, A. Bigos, P. Indyka, and M. Kot, *Surf. Coat. Technol.*, 211 (2012) 67-71.
27. E. Chassaing, K. Vu Quang, M. E. Baumgärtner, M. J. Funk, and C. J. Raub, *Surf. Coat. Technol.*, 53 (1992) 257-265.
28. M. Donten, H. Cesiulis, and Z. Stojek, *Electrochim. Acta*, 50 (2005) 1405-1412.
29. E. O. Hall, *Proceedings of the Physical Society. Section B*, 64 (1951) 747.
30. N. J. Petch, *J. Iron Steel Inst.*, 174 (1953) 25.

© 2015 The Authors. Published by ESG (www.electrochemsci.org). This article is an open access article distributed under the terms and conditions of the Creative Commons Attribution license (<http://creativecommons.org/licenses/by/4.0/>).